

Supplementary Materials for

Tracking Individuals Shows Spatial Fidelity Is a Key Regulator of Ant Social Organization

Danielle P. Mersch,* Alessandro Crespi, Laurent Keller*

*Corresponding author. E-mail: Danielle.Mersch@unil.ch (D.P.M.); Laurent.Keller@unil.ch (L.K.)

Published 18 April 2013 on *Science* Express
DOI: 10.1126/science.1234316

This PDF file includes:

Materials and Methods
Supplementary Text
Figs. S1 to S18
Full Reference List

Other Supplementary Material for this manuscript includes the following: (available at www.sciencemag.org/cgi/content/full/science.1234316/DC1)

Movies S1 to S3

Materials and Methods

Ants

Colonies were initiated from queens collected after a mating flight in March 2007 in Tel Aviv, Israel.

Tracking system

The experimental setup consisted of a nest arena and a foraging arena connected by a tunnel (fig. S1). Each arena was enclosed in a temperature, humidity and light controlled foam box which also comprised a monochrome high-resolution camera (FCi4-14000 monochrome camera, 4560×3048 pixels, Vector international; connected by a Camera Link cable to a mvGAMMA-CL framegrabber (MATRIX VISION) in a computer equipped with an enlarging lens (Rodenstock Rodagon enlarging lens and Rodagon modular focus). To obtain images of workers every half-second we used 5ms long flashes of infrared light (IR) that ants cannot detect (20). The use of flashes had three advantages compared to continuous light exposure. First, it permitted us to use a higher light intensity than under continuous current, which reduced the exposure time and therefore decreased the motion blur of fast moving ants. Second, the short duration of IR flashes greatly decreased residual heating, hence facilitating temperature control in the boxes. Third, high-resolution cameras feature a rolling shutter that needs several milliseconds to read the entire image, thereby creating a time delay between the top and bottom of the image. The use of IR flashes avoided this delay by exposing the entire image at once and reading it subsequently. Because automatic image processing is very sensitive to heterogeneous illumination, the two arenas were lit homogeneously from above by 32 regularly spaced wide-angle IR LEDs. The image exposure was synchronized with the IR flashes by a trigger signal. The camera lens was equipped with an infrared transmitting filter (Hoya IR76 or IR80) to permit constant illumination and thus guarantee a constant detection probability of the tags. Temperature, humidity, light type (UV, visible, IR), light intensity and food supply were regulated by custom made electronic boards and controlled by custom made software. UV and visible lights were used to create a daylight environment for the ants in the foraging arena and in the tunnel, while IR flashes were used in the nest and foraging arena for filming.

Markers

Our tracking relied on markers identified by a feature detection algorithm followed by digital processing. Ants were marked individually with unique matrix codes from the ARTag library (11). These markers consisted of a square outline with a 36-bit digital word encoded in the interior (fig. S2). The digital word can generate up to 2000 unique ID numbers, which are protected from false detection by 26 bits of error correction code (11). The use of markers made the tracking robust to image loss as individuals can be identified unambiguously even if the previous trajectory is unknown or the experiment had been interrupted. The only requirement was that markers are filmed with a resolution of 25–30 pixels per marker side length. For the tested marker size (1.6mm side length) this corresponds to 17–18pixels/mm.

The markers were printed with a laser printer on white paper (180g/m^2) and hand-cut. Each marker weighed approximately 1.4mg. Ants easily carry a weight several times their own (1,21). For *Camponotus fellah* the weight of the markers ranged from 1% of the body weight for the larger workers to 18% for the smaller workers. The markers were fixed on the workers' thorax with Sauer skin glue (Manfred Sauer GmBH, 74931 Lobbach, Germany) while the ant was immobilized by cooling (7°C). The labeled ants recovered within a few minutes when brought back to 28°C . Visual observations suggested that marked ants exhibited normal behavior, except for increased self-grooming behavior in the hour after marking. Marked workers participated in all tasks and interacted with each other and other workers without apparent bias. Their activity levels and resting behavior also appeared similar to that of unmarked ants.

To test whether tags increase the mortality of workers we compared the survival of 100 tagged and 100 untagged workers from one colony kept in a $20\times 30\text{cm}$ fluon painted box. Water and food were provided *ad libitum*. Temperature and humidity were set to 29°C and 50% respectively. Mortality was monitored by counting the number of dead ants of each group every 1–2 days during 4 weeks. The mortality of tagged (12% mortality) and untagged (4% mortality) ants did not differ significantly until day 25 included (day 25: $\chi^2 = 3.3$, df = 1, p = 0.07).

Tracking software

Camera images are processed in real time by a tracker that serves three purposes and that runs on standard commercial computers (Intel Core 2 Quad Q9400, 2.66GHz, 4GB RAM, 2 PCI slots, Gigabit Ethernet). First, it detects and identifies each tag. To increase the probability of tag detection the tracker sharpens and gamma corrects each image. Because the ARTag library can only handle small images, the tracker cuts each image into 15 segments that each overlap by 50 pixels. This overlap is necessary to detect tags that are located on segment borders and would not be detected without the overlap. The tracker sends the image segments to tracking units that scan each segment separately with the ARTag library. The ARTag library searches in each submitted segment for square outlines and compares the content of squares to a list of possible tags (11). If there is a match, the library returns the ID and the coordinates of the four corners of the tag to the tracking unit. The tracking unit calculates the center position and orientation of each detected tag and returns the results to the tracker. When the tracker has received the tracking data from all segments of an image, it writes the result with the corresponding UNIX time (with tenth of second precision) and the image number to a CSV file.

Images are saved as videos to allow later behavioral analyses and to verify manually the quality of our behavior detection algorithms. The video images are resized to 608×912 pixels, compressed with the Xvid codec and saved as AVI files. Each video file covers 2 hours of experiment. The tracker displays the tracking images with the overlaid tracking results on the screen in real time to provide immediate visual feedback

of the tracking quality. The screen display is available ~1s after the image acquisition.

Statistical analyses of 225 immobile (*i.e.*, unattached to ants) reference tags filmed for 12 hours showed that the tags were detected 99% of the time. The (x,y) positions were estimated with mean precision of 2.37 pixels (*i.e.* 0.14mm, ~0.8–2% of a *Camponotus fellah* worker size) and the orientations with a mean precision of 3°. False positives (*i.e.*, detection of a tag where there is none) and erroneous detections of one marker as another marker (inter-marker confusions) were extremely rare ($0.2 \cdot 10^{-7}$). A recording with marked ants showed that tags on live ants were detected with the same precision and accuracy as immobile tags but the detection probability of tags on live ants dropped to $88 \pm 17\%$. As for immobile tags, the probability of false positives and inter-marker confusions was very low ($0.8 \cdot 10^{-7}$). Thus, over 95% of the ants were detected reliably during 1.5 seconds recording time.

Limitations of the tracking system

The tracking system can be used for any species that can be marked with paper tags and kept in a planar arena that can be lit homogenously and filmed. However, there are several challenges. First, some ant species are difficult to mark because they remove or chew the tags. Second some species are difficult to track because individuals sit on top of each other thereby obscuring the tags. Third, smaller species require smaller tags that are more difficult to produce. For small tags (< 0.8mm side length), the resolution of the printing and structure of the paper become very important because the dots in the matrix code need to be well defined (*i.e.* squares instead of circles) to be readable by a computer. We were able to produce readable tags of a size of 0.4mm side length on polymer with offset printing. Fourth, the maximum resolution of a high-resolution camera such as the one we are using can only be reached with high-quality optics. With low quality lenses, the border of the image might be blurry while the center is focused. Finally, the illumination of the arena needs to be very homogenous and constant because low and irregular light intensities result in reduced contrast between white and black dots, making detection unreliable and error prone.

Post-processing

Acquired tracking data were post-processed in six steps to facilitate subsequent behavioral analyses (steps one, two and four were performed separately for the data obtained from the cameras in the nest and foraging arenas). First, image data were ordered sequentially and double detections in the same image were removed. Second, we removed cases of inter-marker confusions that could be detected on immobile ants (*i.e.* there is an initial change of location and orientation of the tag followed by a return to the original position and orientation). Third, to determine the orientation of each ant, we manually measured on the images for each individual the angle difference between the front of the tag and the front of the ant (fig. S3), and then corrected all angles in the tracking data. Fourth, we determined whether an undetected tag corresponds to an ant that had left the arena and entered the tunnel or an ant that remained undetected in the

arena. A suite of four criteria identifies ants that entered the tunnel: *i.* the last detection of the tag must be in an 18×12mm area adjacent to the arena exit; *ii.* the last recorded movement or orientation of the tag must be directed towards the arena exit; *iii.* the tag must remain undetected for at least three seconds; *iv.* upon redetection, the tag's orientation and position must differ by more than 25° and 0.3mm from that of the previous detection. Fifth, the data frames from the nest and foraging arena cameras were merged and verified at each time point to make sure a tag was only detected in a single arena. If a tag was simultaneously detected in both arenas, only the position that minimizes the distance to its previous detection was retained. Sixth, the data were screened to discriminate between live marked ants and dead marked ants, and between live marked ants and tags that were lost and lay on the ground. Because workers sometimes carry dead marked ants and lost tags it is difficult to distinguish them from living marked ants. Therefore, we used a data set of 68 ants whose death dates were determined visually from the videos to heuristically identify criteria that distinguished dead ants from ants that were alive and marked. Ants were considered dead (and their time of death was recorded), if they fulfilled at least one of the following three criteria: first, there were more than 259 5-minute intervals in which the maximal distance of the tag to its first detection in the interval was less than 18mm, or second, there were more than 518 5-minute intervals during which the tag was undetected, or third, the tag was completely immobile for more than 43 5-minute intervals and remained undetected in more than 22 5-minute intervals.

To avoid erroneously considering a marked ant as dead, we recorded an ant as alive and marked if the tag satisfied one or more of three heuristically determined conditions: first, there were more than 20 5-minute intervals during which the sum of the distances moved by the tag was more than 6mm, or second, there were more than eight intervals during which the maximal distance of the tag to its first detection in the interval exceeded 180mm, or third, the tag was detected in at least 60 distinct 5-minute intervals.

Interaction detection

To automatically infer interactions we jointly considered three parameters: the distance between two ants, the angle between their bodies, and the time spent nearby. Two individuals interacted if the angle between their bodies was greater than 70°, and if they were more than 1 second in a position where at least one ant could reach the body of the other ant with its antennae (fig. S4). Most ant pairs whose orientations differed by less than 70° (*i.e.* ants that tended to be parallel and faced the same direction) were unlikely to interact, and we therefore excluded these interactions to minimize false positives. To account for variable sizes of the ants, we estimated for each ant the distance between the center of its tag and the center of the tips of the antennae when they were bended in a 90° angle (fig. S4A). This distance is referred to as antennae reach, and the center of the antennae tips is referred to as interaction point. The body of each ant was modeled by a trapezoid of length 2.0 * antennae reach, of width 0.35 * antennae reach at

the abdomen end of the trapezoid, of width $0.45 * \text{antennae}$ reach at the head end of the trapezoid, and centered on the ant's position. These three coefficients were estimated heuristically from a data set where more than 100 interactions were visually determined. We varied the three coefficients between zero and three in intervals of 0.01 and selected the three values providing the best fit with the visually inferred interactions. Using these coefficients we estimated the number and duration of interactions by identifying the time steps in which the interaction point of one ant was within the trapezoid of the other ant (fig. S4B-D).

Interactions between two ants can only be detected with our criteria if both ants are detected at the same time. Therefore, to combine interactions that correspond to a single interaction event lasting for several images, we grouped subsequent interactions together when they were no more than 10 seconds apart, and if the interacting individuals had moved less than 2mm and changed their orientations by less than 20° . Interactions that lasted less than a second after grouping were discarded, because they could simply result from two ants that passed near each other without interacting.

Social network analysis

For each day and each colony we built a social network by cumulating all interactions over the day. In the constructed networks almost all ants interacted with all other ants, hence producing very dense networks (colony mean density: $72 \pm 5.3\%$). Because community detection algorithms fail with such highly connected networks (22), we reduced the network density (*i.e.*, proportion of edges in the network relative to the total number of edges possible) of each network to approximately 25% ($24.6 \pm 5.8\%$) by removing the edges that had the smallest number of interactions. Filtered networks were submitted to the Infomap community detection algorithm (13), which determines based on a random walk combined with data compression how many distinct clusters are present in a network, and assigns each ant to a single cluster. The idea behind the algorithm is that nodes and edges in a network represent a map of connections that guide and constrain information flow, and that the speed at which information flows across those connections indicates which nodes are highly connected (*i.e.* form a cluster). Over the 11 first experimental days and also in all three subsequent 10-day periods most workers were assigned to more than one cluster, which can result from noisy and erroneous cluster assignments or reflect gradual group transitions. Therefore, we generated a single group affiliation by combining cluster assignments over the first 11 days and each further 10-day period. To account for some variability and error in daily cluster assignments, we affiliated ants to the cluster-group in which they spent at least 70% of their time (*i.e.*, 8 out of 11 days, or 7 out of 10 days). Ants that spent less than 8 or 7 days, respectively, in a given cluster were grouped together in a distinct third group as shown in fig. S5. The 70% threshold is arbitrarily chosen, but results do not differ qualitatively if lower (60%) or higher thresholds (80%) are used.

Probability of random interactions

To test whether the observed social structure could arise from simple differences in the rate of interactions among the three groups of workers, we compared the observed interaction frequency to the theoretical frequencies derived from the relative proportion of interactions of nurses, cleaners and foragers. These analyses revealed that there were 2.3–2.9 times more interactions within groups than predicted under random interactions (nurses (N): Kruskal-Wallis (KW): $\chi^2 = 502.8$, $p = 2.3 \cdot 10^{-111}$, cleaners (C): KW: $\chi^2 = 329.5$, $p = 1.2 \cdot 10^{-73}$, foragers (F): KW: $\chi^2 = 348.9$, $p = 7.4 \cdot 10^{-78}$, fig. 1B).

Spatial distribution of ants and probability of interactions

To determine the spatial distribution of workers of the three groups (nurses, cleaners and foragers) we divided the nest arena in a grid of 46×31 cells (cell size: 6mm×6mm) and calculated the frequency with which workers of each group visited each cell. These frequencies are the probabilities with which a worker visiting the cells will interact with workers of the three groups if the spatial distribution affects the social structure. For every worker we therefore identified the cells visited during the first 11 days of the experiment and then averaged the cell- and group-specific interaction probabilities. Because a worker cannot interact with itself, we excluded its visits from the cells when calculating the group-specific interaction probability. The cell- and group-specific interaction probabilities were estimated on a daily basis because the spatial distribution of workers slightly changed over days. Because workers of the three groups differed in their overall interaction frequency, we normalized the probability by the group specific interaction frequency. The predicted interaction frequencies were robust to changes in cell size, lack of normalization, and shorter or longer estimation intervals.

Information spread

To determine the rate at which information could spread in the colony, we randomly selected in each colony and in each group (nurses, cleaners, foragers) nine individuals as information carriers, and then determined the speed at which the information spread to workers of the three groups. Because colony and group activity levels are likely to affect the speed of information spread, we estimated information spread at 9 different time points during the first 10-day period, and selected for each time point three ants (one from each group) as information carrier. The speed of the spread was estimated from the time of the first interaction of the information carrier until all workers were informed either directly by the information carrier or by other ants that had interacted with the information carrier. We tested whether workers transmit information faster to workers of their own group than to workers of other groups with a Cox proportional hazard model using generalized estimating equations with colonies as clusters.

Supplementary Text

Analysis of the interactions between groups

To confirm the results from the network analysis and determine whether group three, which was created by grouping all remaining workers that were not affiliated with group one or two corresponded to a social group, we compared for each group the within-group interaction frequency to the between-group interaction frequency. As inferred from the network analysis workers interacted 2.1 ± 0.6 times more often with members of their group than with members from other groups (KW: $\chi^2=272.6$, $p<10^{-60}$). Workers of the first group interacted 5.9 ± 2.5 times more often with their group members than with workers of the second group and 2.1 ± 0.3 times more often than with workers of the third group (KW: $\chi^2=556.7$, $p < 10^{-111}$, post-hoc comparisons: $p_{G1-G2} < 10^{-308}$, $p_{G1-G3} < 10^{-57}$; fig. 1B). Workers of the second group interacted 2.4 ± 0.8 times more often with their group members than with workers of the third group, and 7.9 ± 3.1 times more often than with workers of the first group (KW: $\chi^2=597.9$, $p < 10^{-119}$, post-hoc comparisons: $p_{G2-G3} < 10^{-51}$, $p_{G2-G1} < 10^{-308}$; fig. 1B), while workers from the third group interacted 1.5 ± 0.4 times more often with members of their own group than with workers from the first group and 1.4 ± 0.3 times more often than with members of the second group (KW: $\chi^2 = 223.8$, $p < 10^{-40}$, post-hoc comparisons: $p_{G3-G1} < 10^{-33}$, $p_{G3-G2} < 10^{-15}$; fig. 1B). The significantly higher frequency of within-group interactions for workers of the third group confirmed that their group is not an artifact of the 70% threshold used for grouping but that they indeed form a distinct social group. Workers from the third group required less time to interact with 80% of all workers in a colony than workers from the other two groups (KW: $\chi^2=83.8$, $p < 10^{-12}$). Because workers of the third group had 12% lower interaction frequencies (KW: $\chi^2=17.6$, $p < 10^{-3}$), the time difference between groups in the 80% contact rate highlights that workers from the third group are more connected to other workers than workers from the first and second group.

Group transitions

Overall, $13.2 \pm 6.0\%$ of the nurses switched groups with most transitions occurring to the cleaner group. Switching nurses were 5.4 ± 4.9 times more likely to become a cleaner than a forager (KW: $\chi^2=11.56$, $p=0.003$). The percentage of cleaners switching groups was significantly higher ($43.4 \pm 15.5\%$, KW: $\chi^2=11.23$, $p=0.0036$), with 7.5 ± 5.8 more transitions to the foraging group than to the nurse group (KW: $\chi^2=13.35$, $p=0.001$). Finally, only $8.2 \pm 5.2\%$ of the foragers switched groups and $95.8 \pm 10.2\%$ of the transitions occurred to the cleaning group (KW: $\chi^2=15.82$, $p=4.0 \cdot 10^{-4}$). These results show that workers exhibit a preferred behavioral trajectory moving from nursing to cleaning to foraging as they age.

Age-related division of labor in ants

While it is commonly believed that there is an age-related division of labor in ants, there is actually only relatively weak support for this claim. First, and most importantly, worker age has been generally inferred from indirect evidence such as cuticular color, mandibular wear, or ovarian development. These methods are generally accurate for

young individuals (*e.g.*, younger than 20 days) but less so for older individuals (older than 20 days), which limits the extent to which age-related division can be inferred. Second, worker behavior is typically assessed only once over a few hours, thus further limiting the possibilities of detecting age-related division of labor. Overall, these studies show that age-related division of labor exists in some ant species but not in others (reviewed in 1), and that for a given species the conclusions about age-related division of labor can differ between studies (14). Of all these studies, only one tracked changes in behavior as workers age. In this study, Lenoir (15) showed that, among the 40 workers that were individually marked and whose behavior was observed over 40 days, only 50% exhibited age-related transitions.

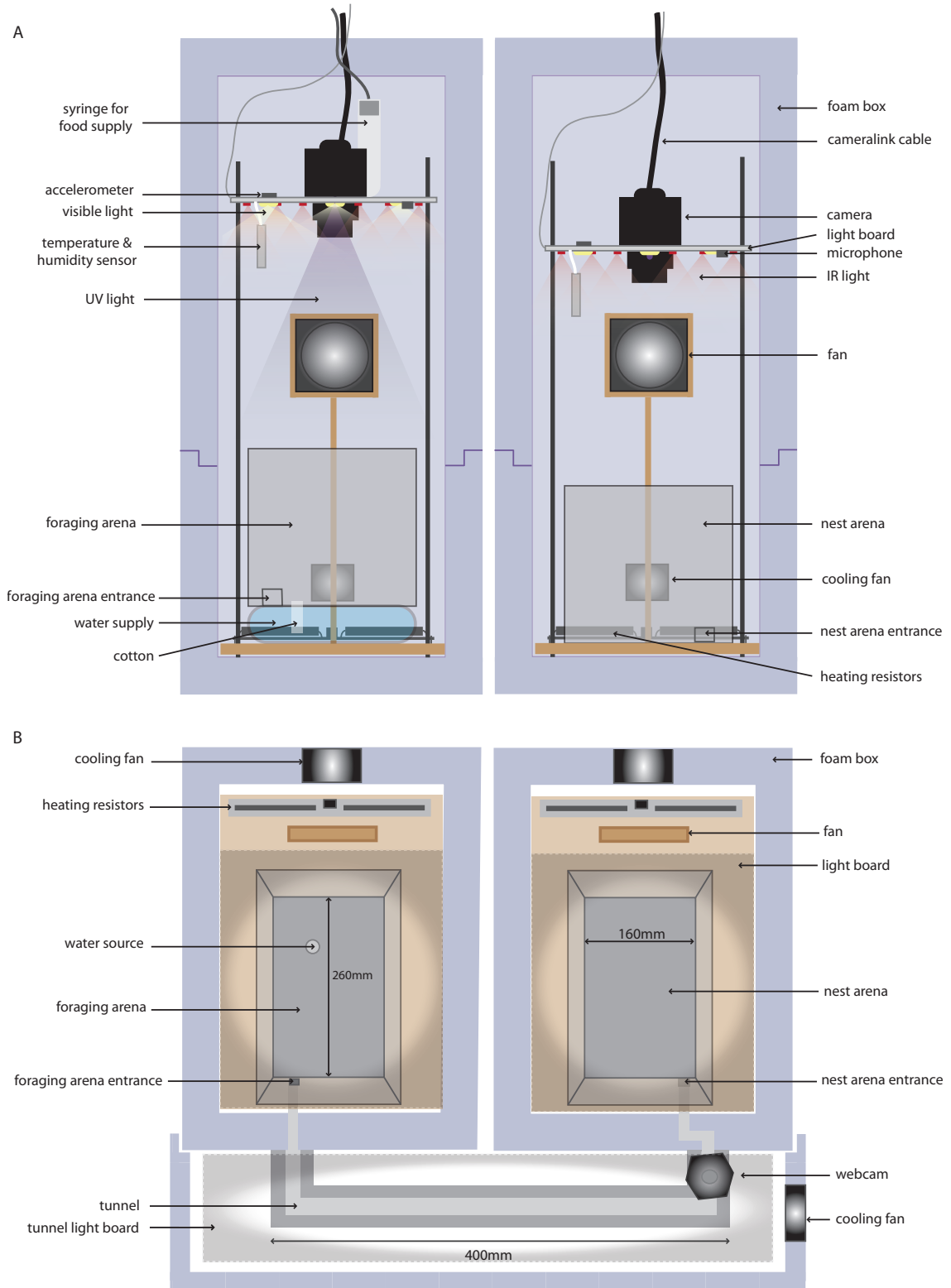
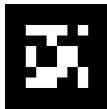


Fig. S1.

Tracking setup **(A)** Lateral view **(B)** Top view.



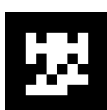
Tag 37



Tag 4



Tag 57



Tag 478



Fig. S2.

Example of ARTag markers and marked ants. Photo by Dr. Joël Meunier.

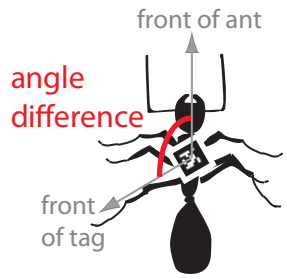


Fig. S3.

Angle difference between the front of the tag and the front of the ant.

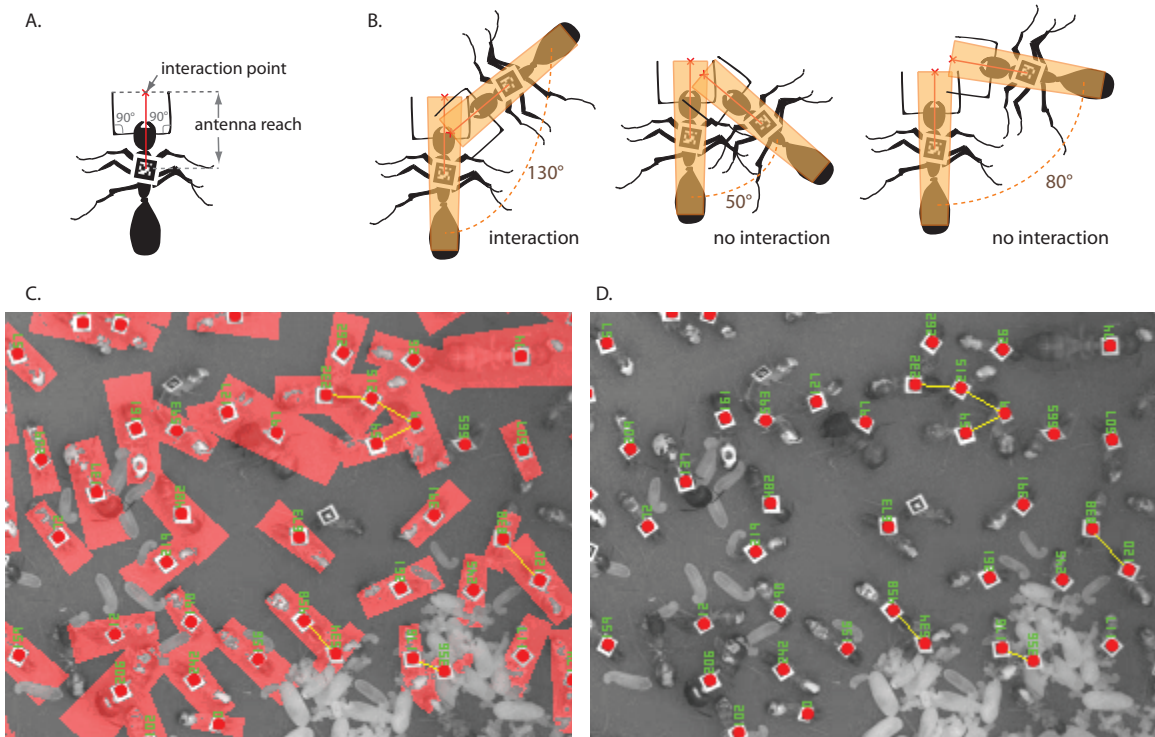


Fig. S4.

Interaction detection **(A)** Antennae reach distance and interaction point **(B)** Trapezoid modeled to represent the ants and inferred interactions **(C)** Trapezoids overlaid on real ants **(D)** Detected interactions (yellow lines).

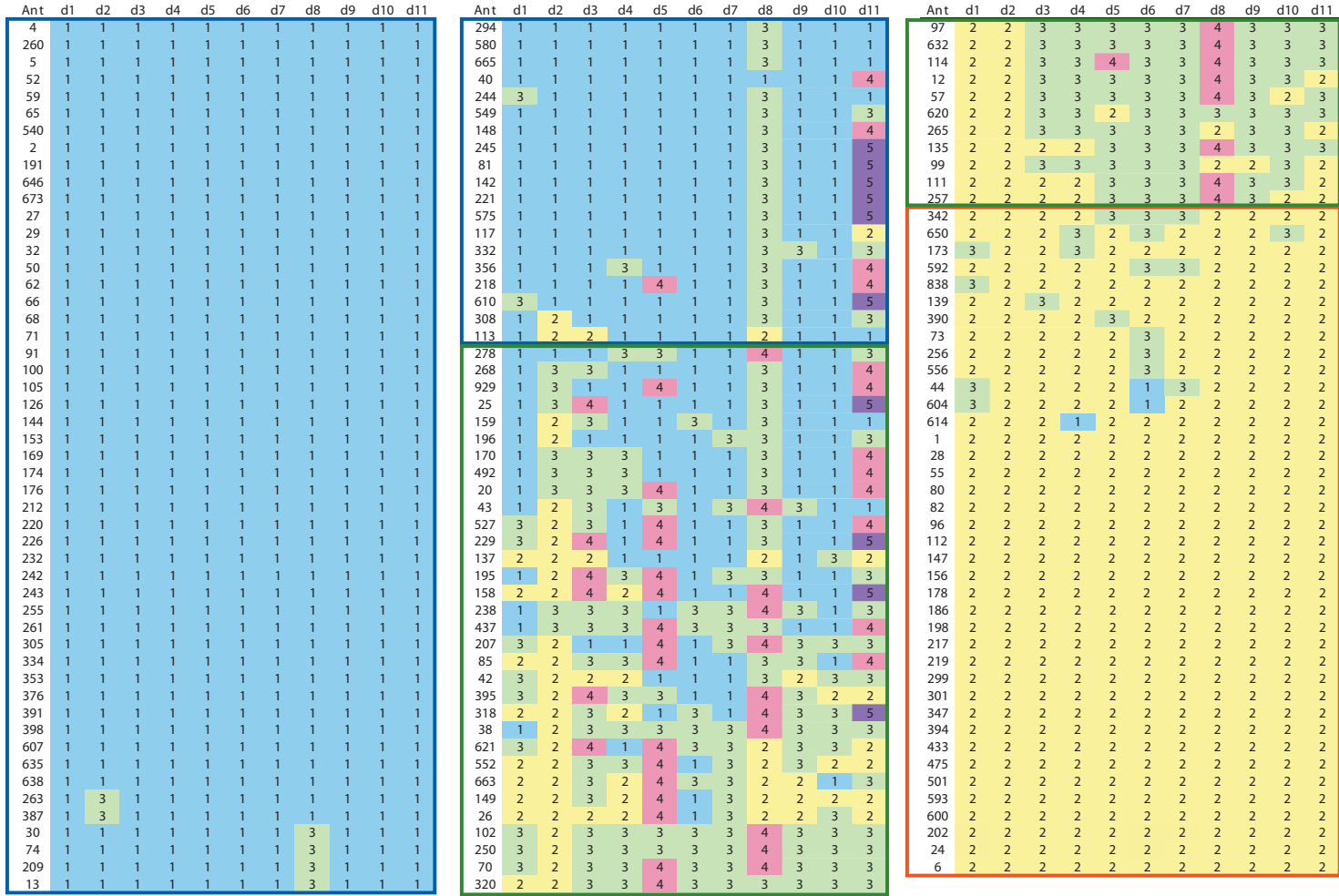


Fig. S5.

Daily cluster assignments of all ants of colony 5 over the first 11-day period of the experimental data. Each color indicates a different cluster membership. Each row corresponds to an ant and each column to a day. The square outlines indicate the group affiliation: nurses (cluster 1 outlined in blue), foragers (cluster 2 outlined in orange) and cleaners (remaining ants grouped in clusters 3 outlined in green).

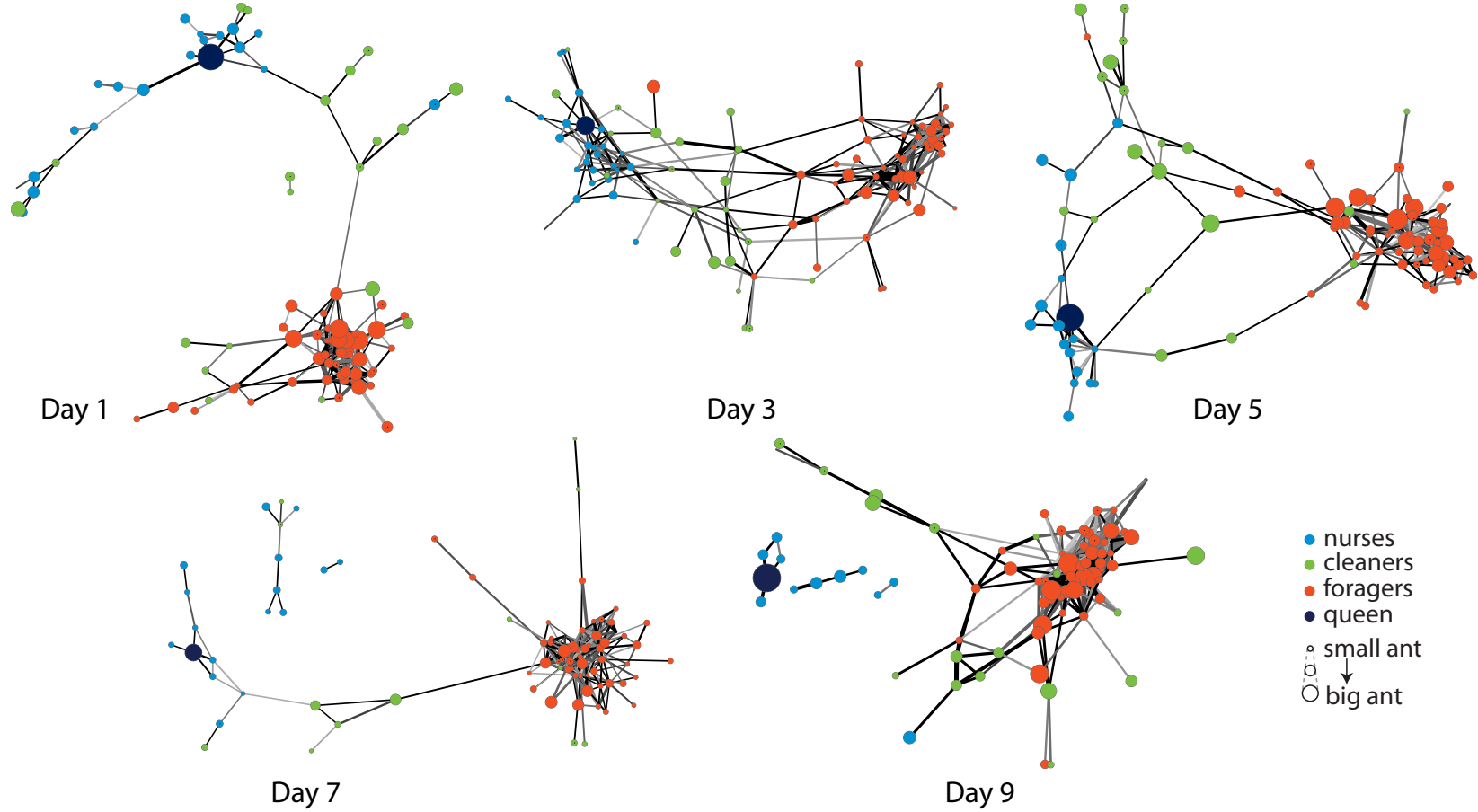


Fig. S6.

Social networks of colony 1 on days 1, 3, 5, 7 and 9 of the experiment. Edge width is proportional to the number of interactions between pairs of nodes. The darkness of edges is proportional to the average duration of interactions. The network is laid out with the spring embedded layout from Cytoscape (19). For visual purposes only edges of ant pairs that interacted more than 20 times are shown. Ants that became isolated after this edge filtering (17–48 workers depending on days and colonies) are not plotted.

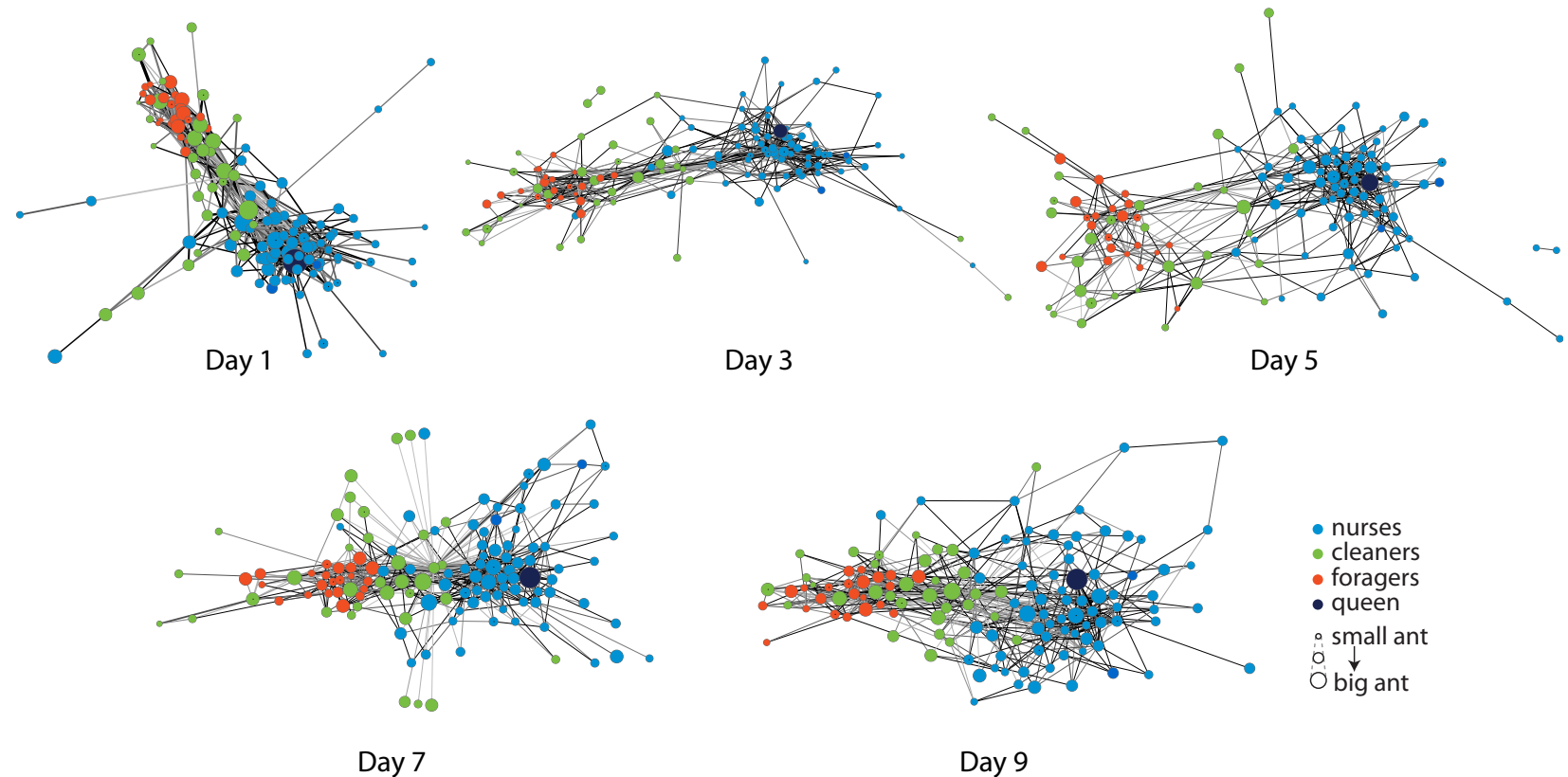


Fig. S7.

Social networks of colony 2 on days 1, 3, 5, 7 and 9 of the experiment. Edge width is proportional to the number of interactions between pairs of nodes. The darkness of edges is proportional to the average duration of interactions. The network is laid out with the spring embedded layout from Cytoscape (19). For visual purposes only edges of ant pairs that interacted more than 20 times are shown. Ants that became isolated after this edge filtering (17–48 workers depending on days and colonies) are not plotted.

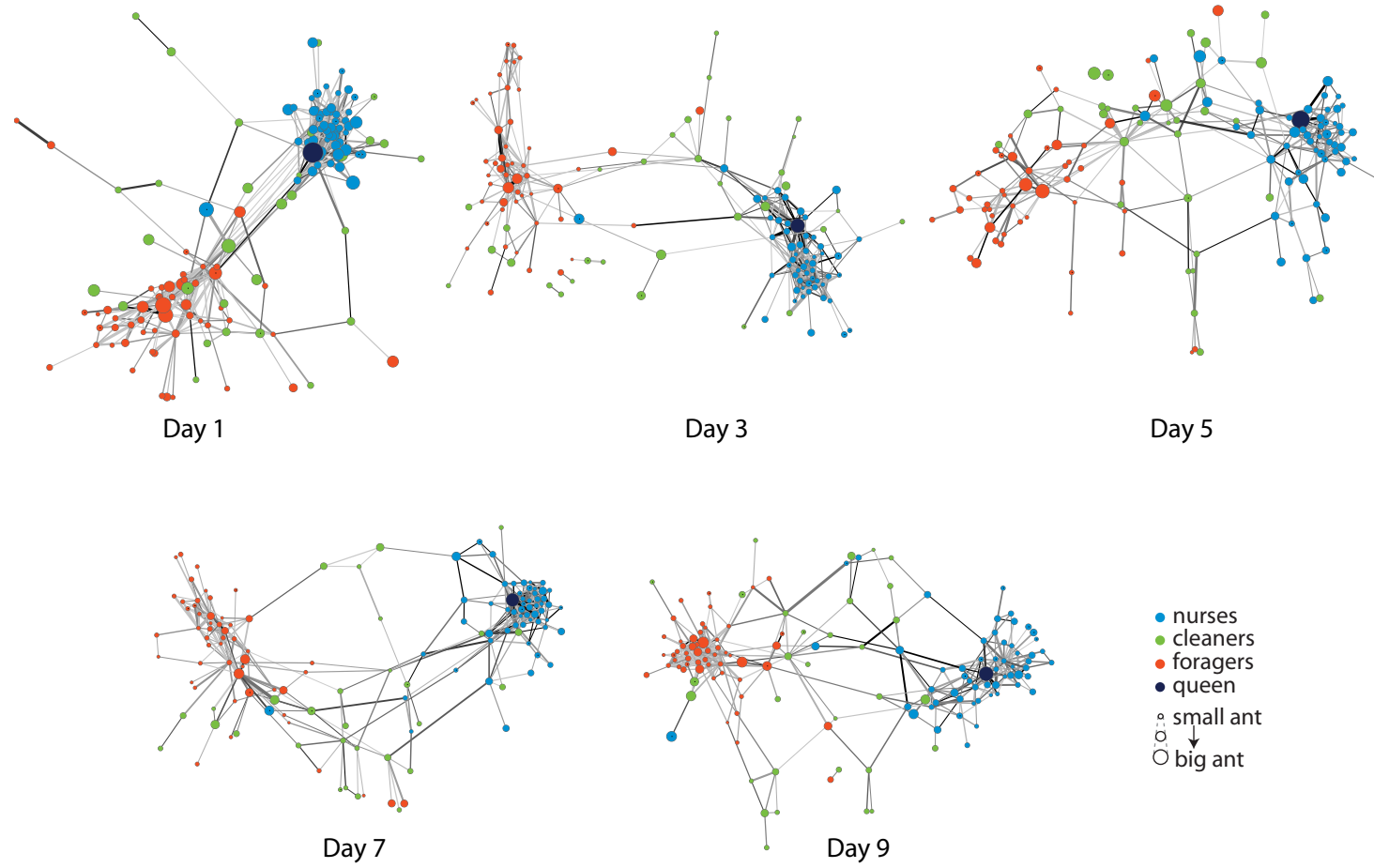


Fig. S8.

Social networks of colony 3 on days 1, 3, 5, 7 and 9 of the experiment. Edge width is proportional to the number of interactions between pairs of nodes. The darkness of edges is proportional to the average duration of interactions. The network is laid out with the spring embedded layout from Cytoscape (19). For visual purposes only edges of ant pairs that interacted more than 20 times are shown. Ants that became isolated after this edge filtering (17–48 workers depending on days and colonies) are not plotted.

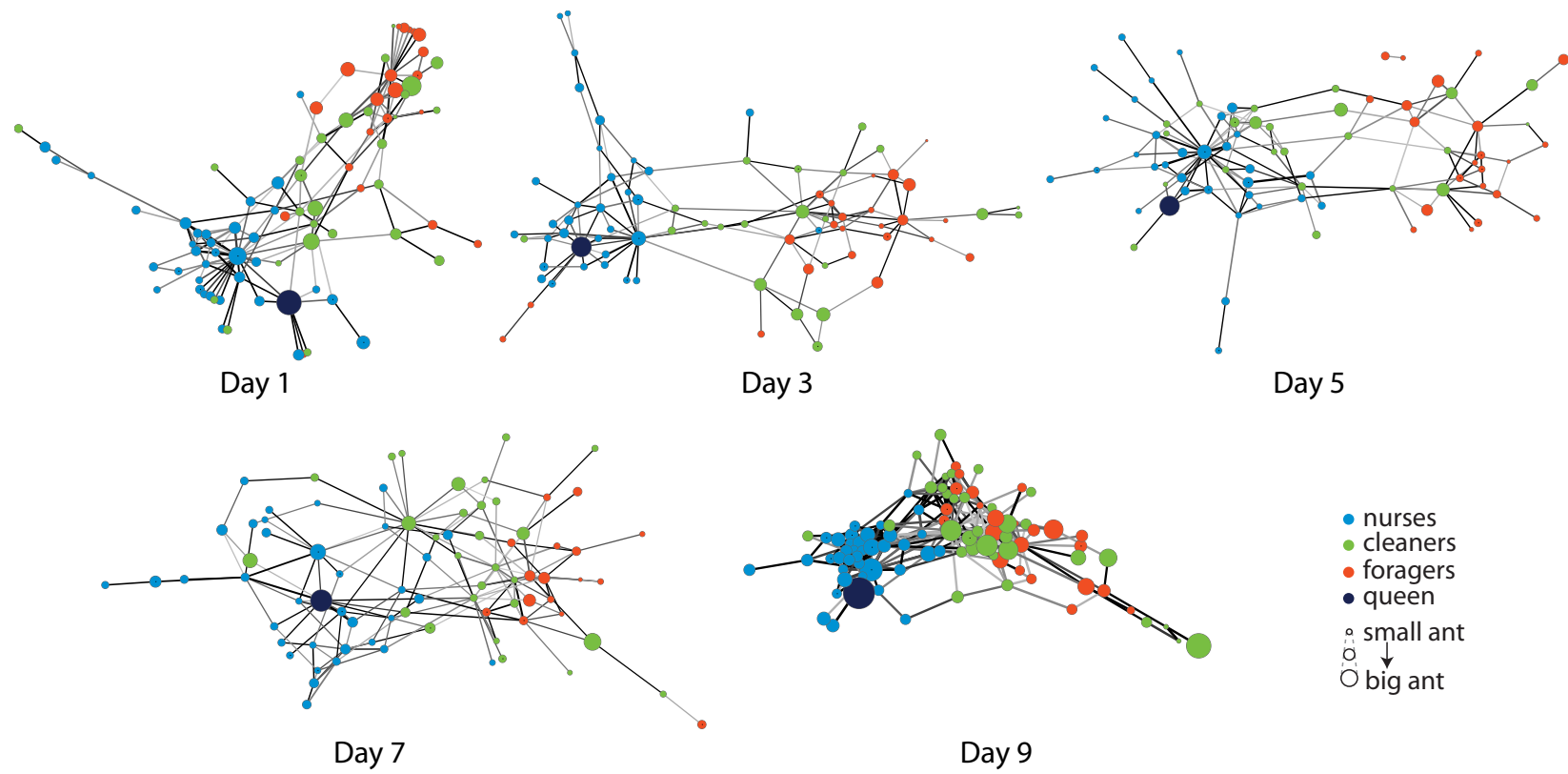


Fig. S9.

Social networks of colony 4 on days 1, 3, 5, 7 and 9 of the experiment. Edge width is proportional to the number of interactions between pairs of nodes. The darkness of edges is proportional to the average duration of interactions. The network is laid out with the spring embedded layout from Cytoscape (19). For visual purposes only edges of ant pairs that interacted more than 20 times are shown. Ants that became isolated after this edge filtering (17–48 workers depending on days and colonies) are not plotted.

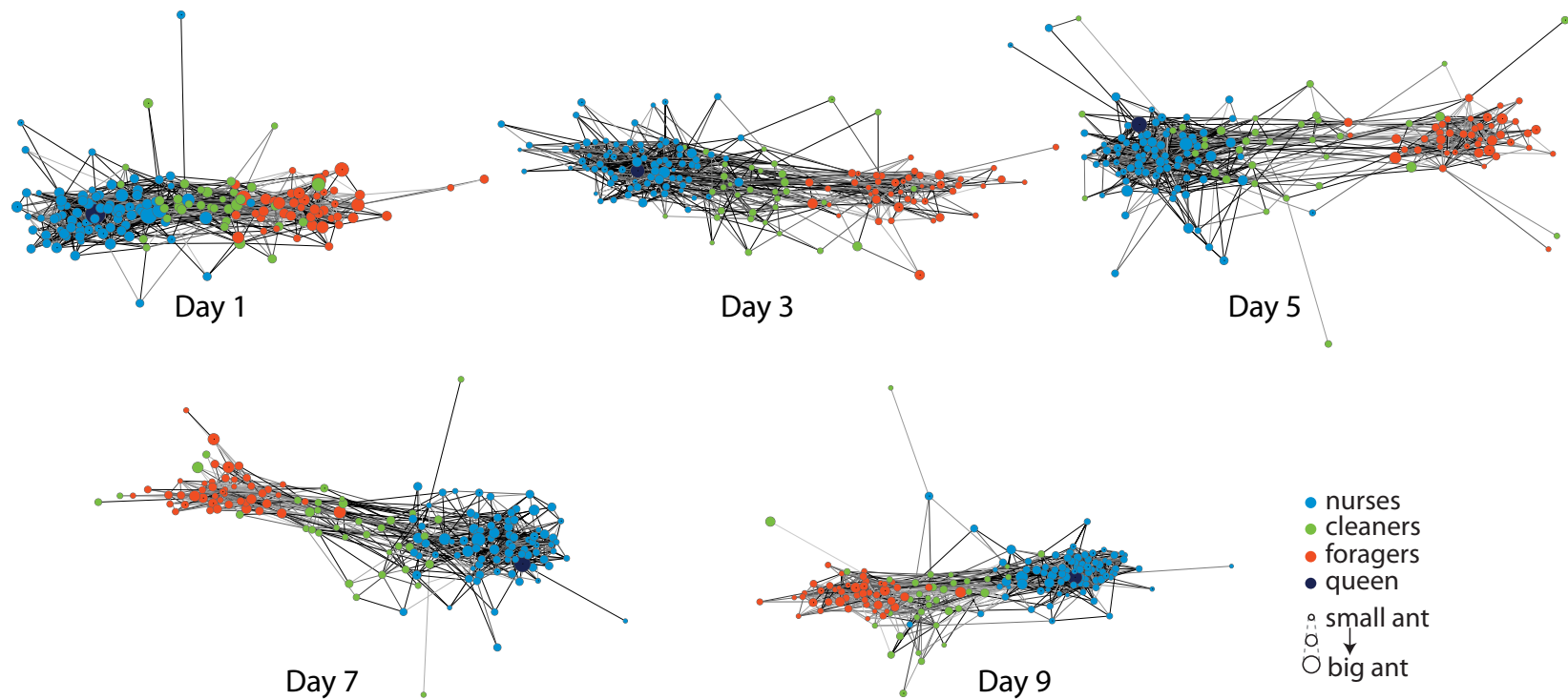


Fig. S10.

Social networks of colony 6 on days 1, 3, 5, 7 and 9 of the experiment. Edge width is proportional to the number of interactions between pairs of nodes. The darkness of edges is proportional to the average duration of interactions. The network is laid out with the spring embedded layout from Cytoscape (19). For visual purposes only edges of ant pairs that interacted more than 20 times are shown. Ants that became isolated after this edge filtering (17–48 workers depending on days and colonies) are not plotted.

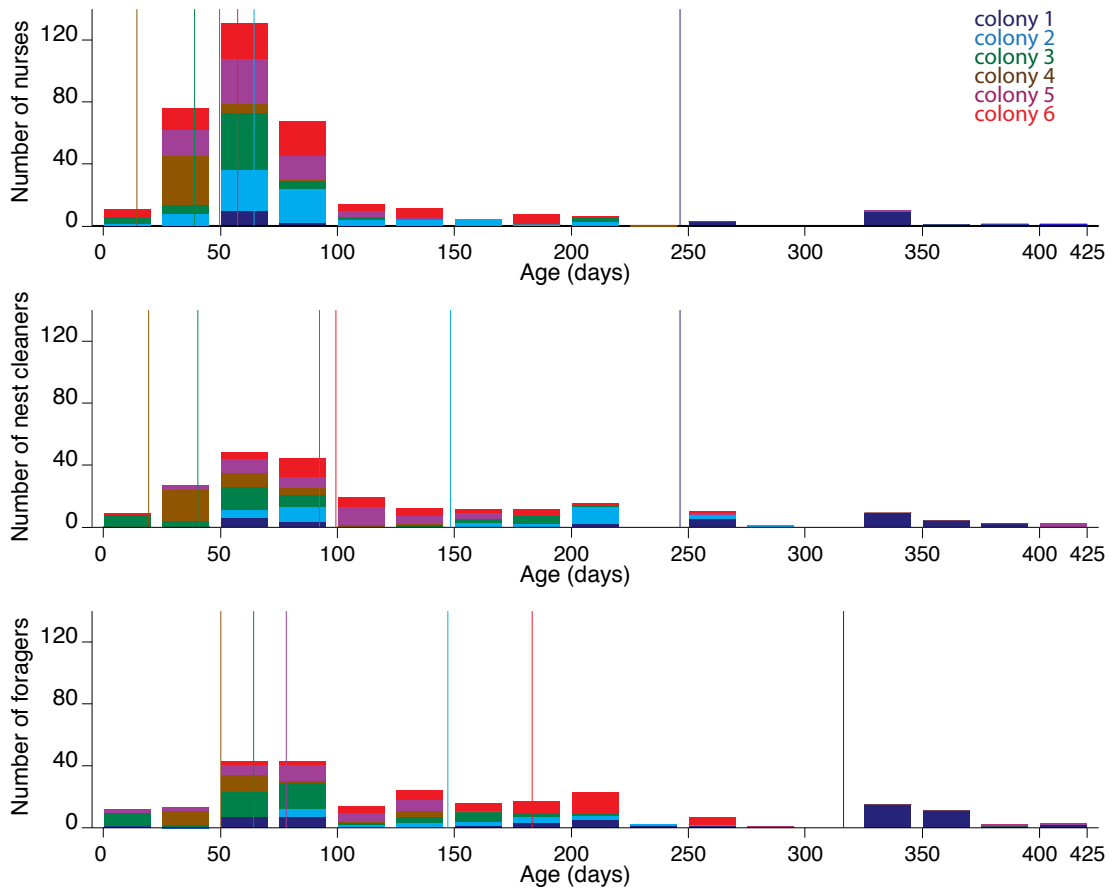


Fig. S11.

Age distribution of each worker group. Colors indicate different colonies. Vertical lines indicate colony medians.

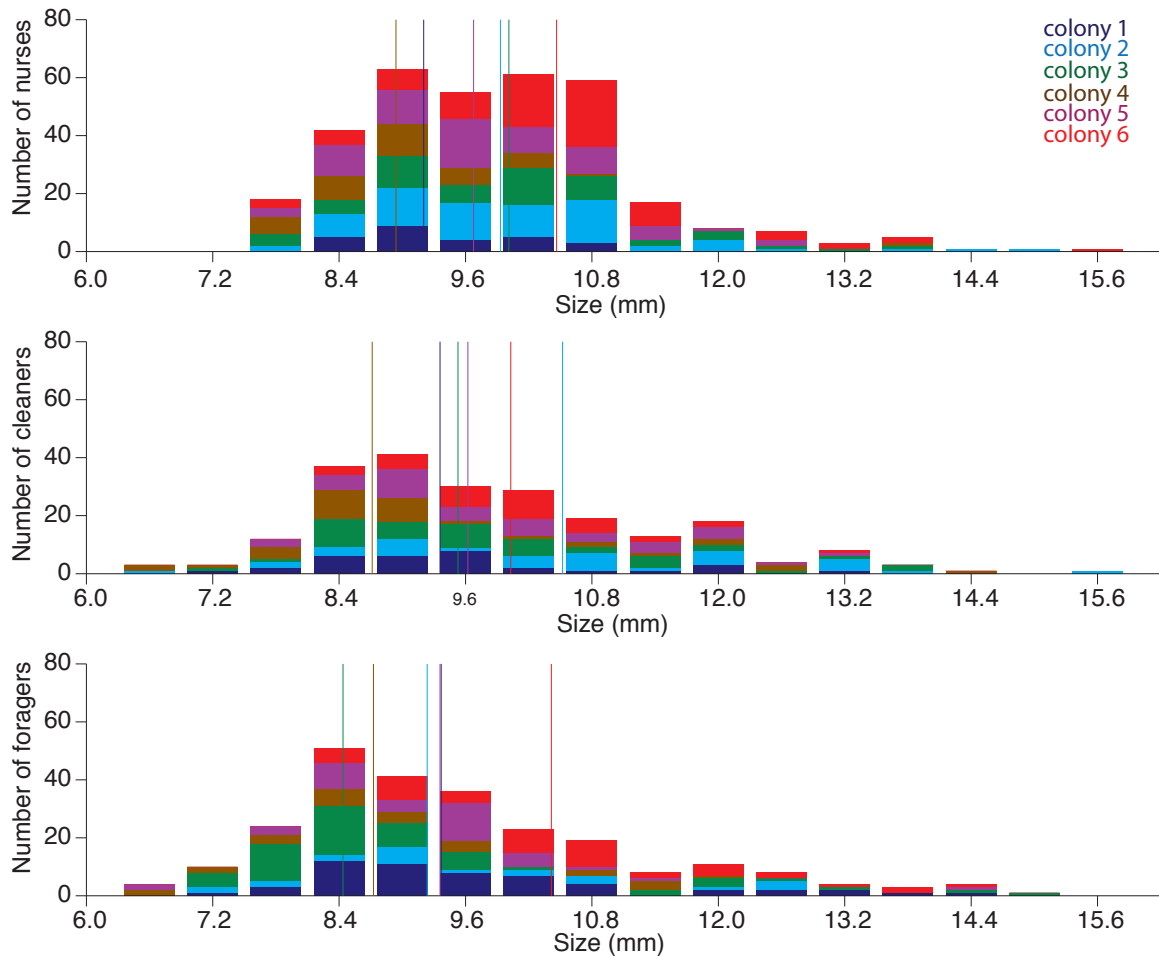


Fig. S12.

Size distribution of each worker group. Colors indicate different colonies. Vertical lines indicate colony medians.

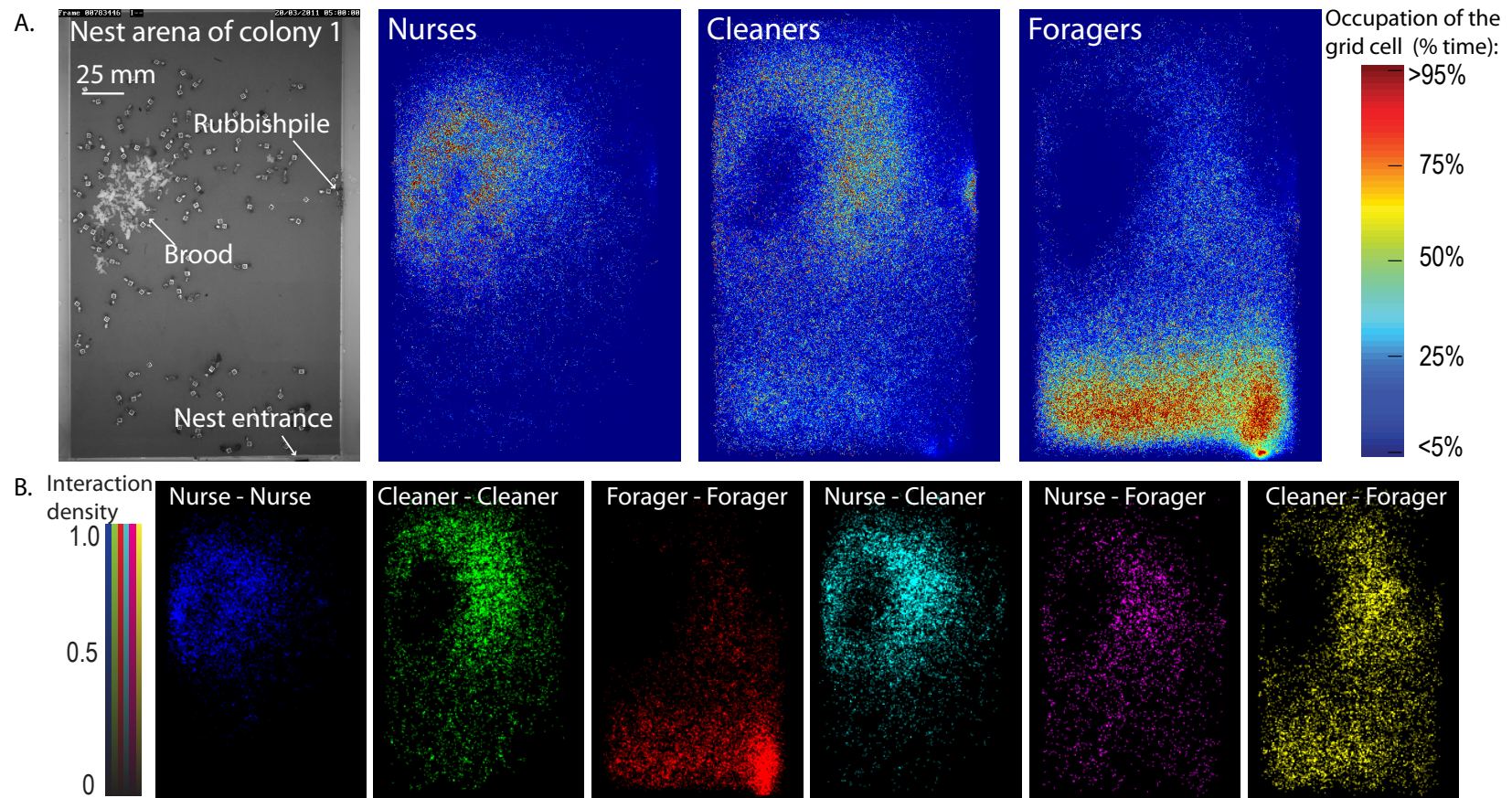


Fig. S13.

Spatial distributions of colony 1. **(A)** Spatial organization of the nest and spatial distribution of nurses, cleaners and foragers. **(B)** Spatial distribution of within- and between-group interactions.

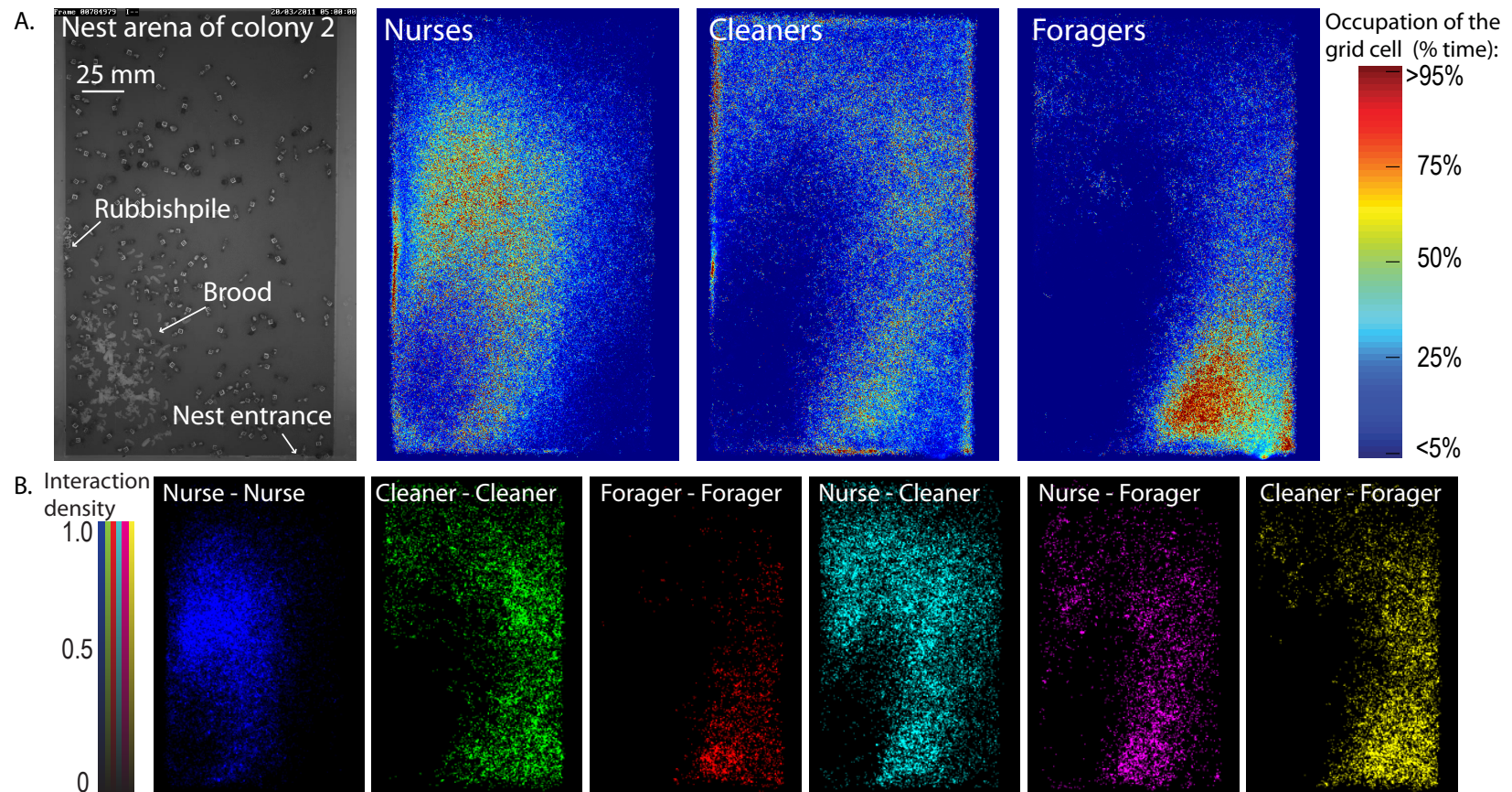


Fig. S14.

Spatial distributions of colony 2. **(A)** Spatial organization of the nest and spatial distribution of nurses, cleaners and foragers. **(B)** Spatial distribution of within- and between-group interactions.

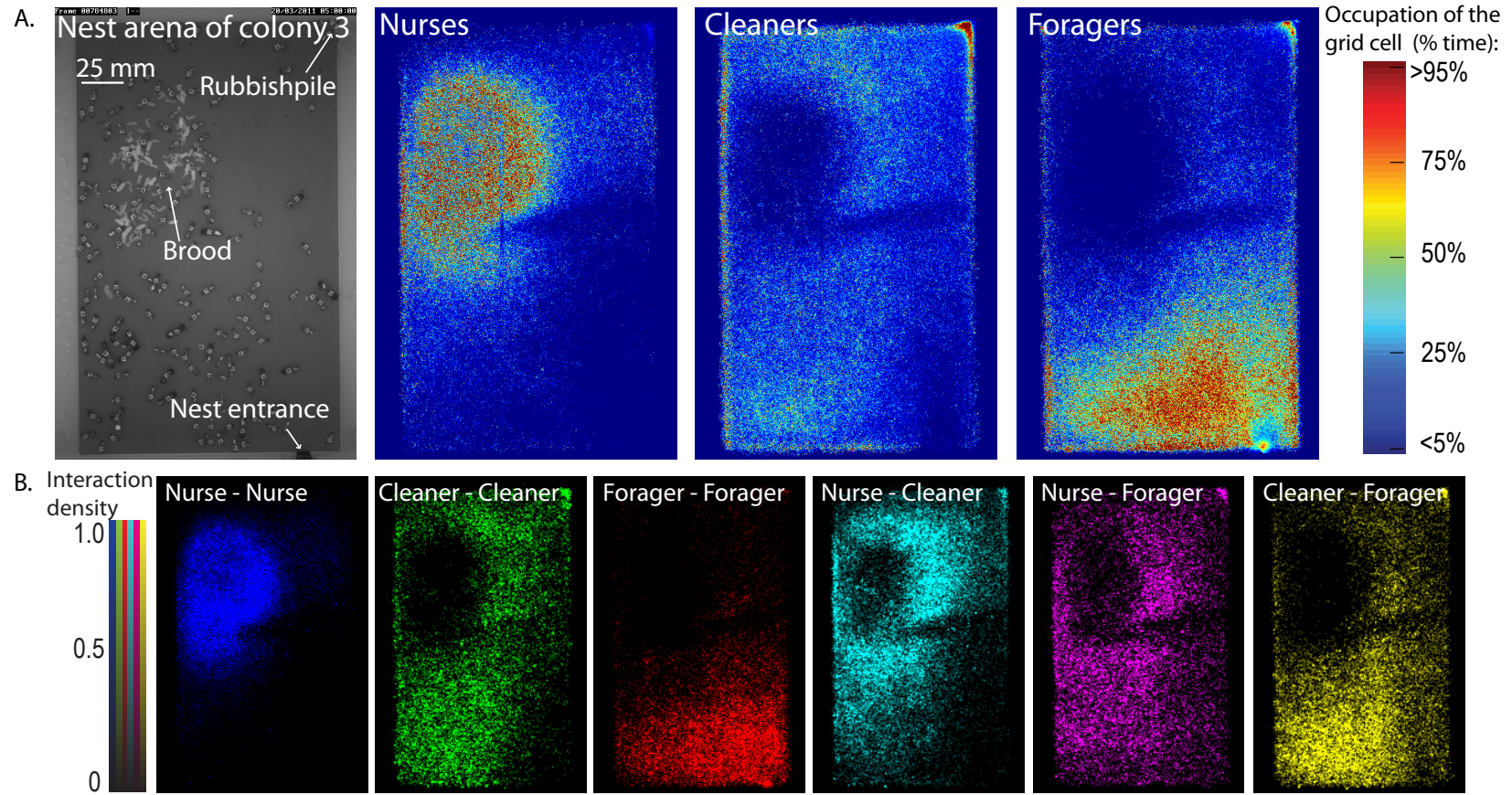


Fig. S15.

Spatial distributions of colony 3. **(A)** Spatial organization of the nest and spatial distribution of nurses, cleaners and foragers. **(B)** Spatial distribution of within- and between-group interactions.

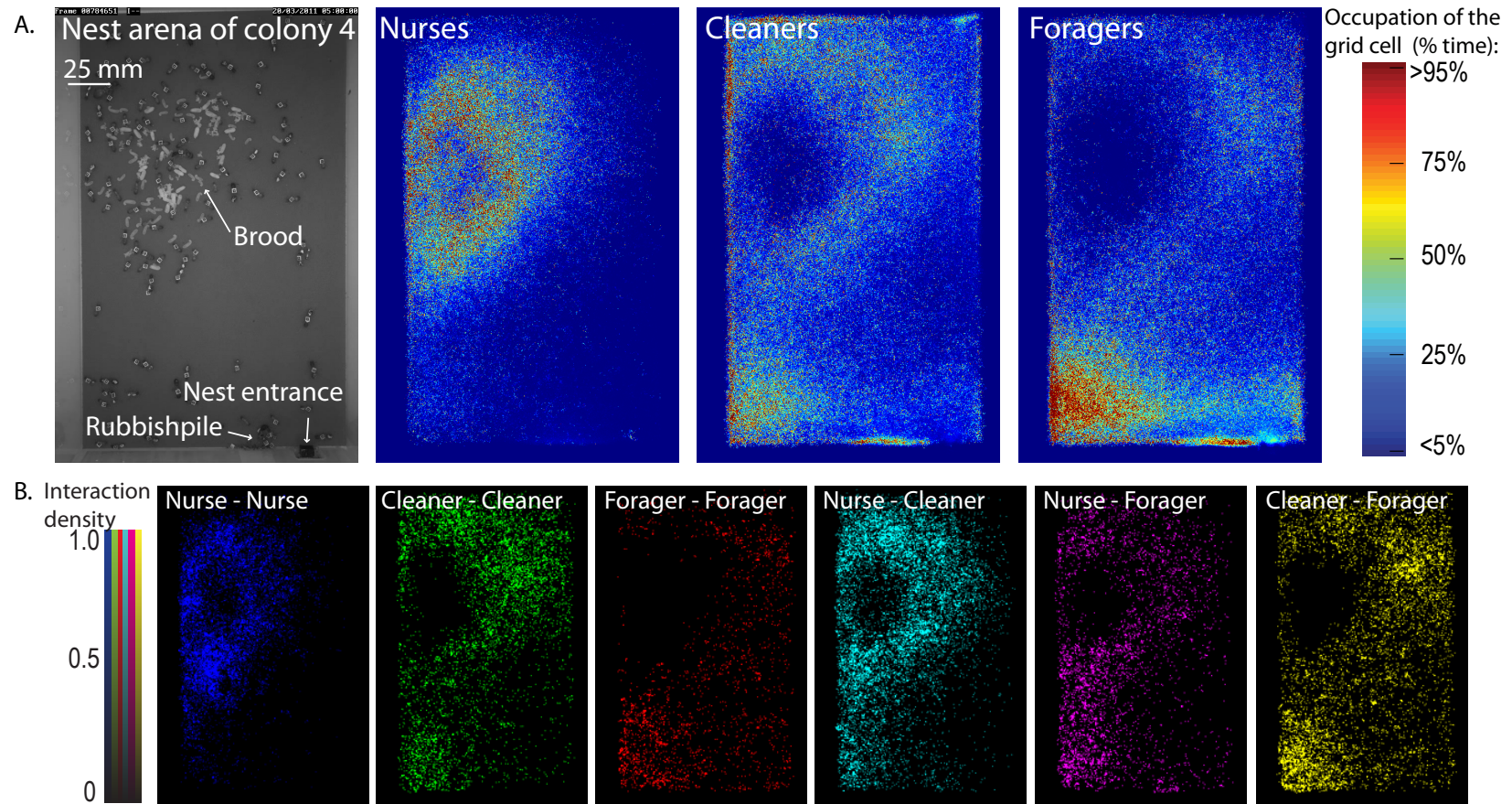


Fig. S16.

Spatial distributions of colony 4. **(A)** Spatial organization of the nest and spatial distribution of nurses, cleaners and foragers. **(B)** Spatial distribution of within- and between-group interactions.

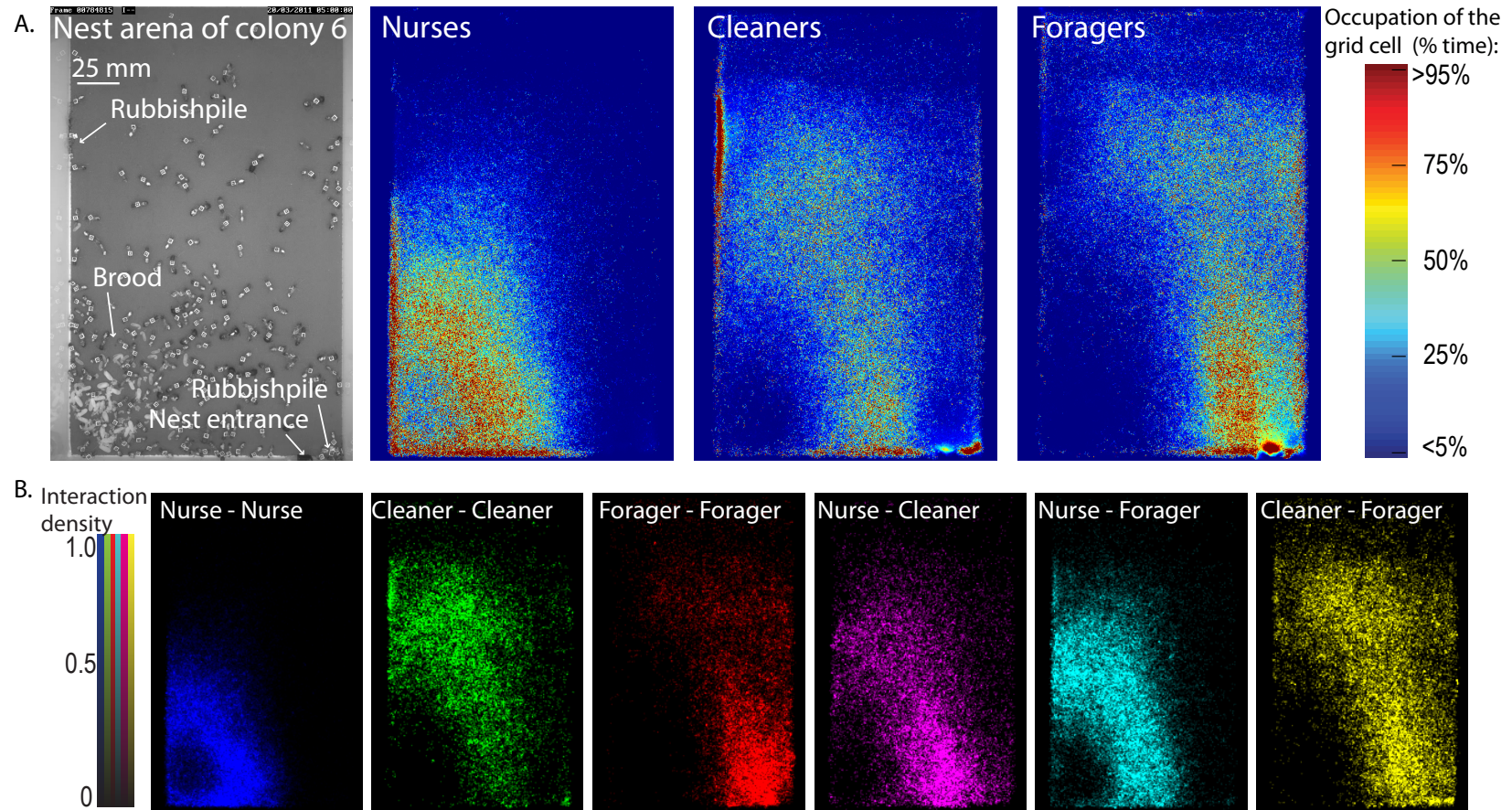


Fig. S17.

Spatial distributions of colony 6. **(A)** Spatial organization of the nest and spatial distribution of nurses, cleaners and foragers. **(B)** Spatial distribution of within- and between-group interactions.

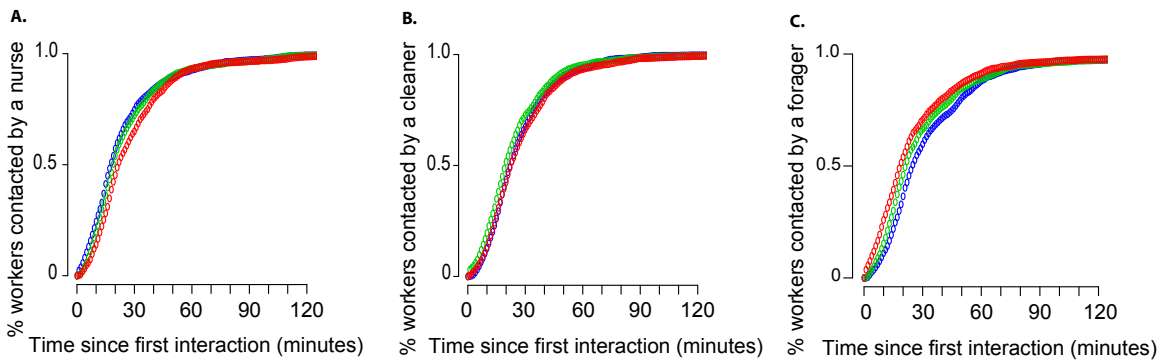


Fig. S18.

Information spreads faster within groups than between groups when (A) nurses and (C) foragers emit information, but not when (B) cleaners emit information. Receiver groups: blue (nurses), green (cleaners), orange (foragers). Every circle represents the average of 54 individuals from six colonies.

Movie S1

Detected ants in the nest arena and their trajectories in the minute preceding the current detection. The frame rate is accelerated 5 times.

Movie S2

Interactions between ants in the nest arena are marked by yellow lines. The frame rate is accelerated 5 times.

Movie S3

Spread of information in a colony. The information spread is initiated from ant 217 (blue tag, top right corner in the movie). All ants that directly or indirectly interacted with ant 217 become informed (blue color). The frame rate is accelerated 5 times during the first 15 seconds, then 10 times in the next 20 seconds and 20 times for the remaining time.

References and Notes

1. B. Hölldobler, E. O. Wilson, *The Ants* (Springer, Berlin, 1990).
2. G. E. Robinson, Regulation of division of labor in insect societies. *Annu. Rev. Entomol.* **37**, 637 (1992). [doi:10.1146/annurev.en.37.010192.003225](https://doi.org/10.1146/annurev.en.37.010192.003225) [Medline](#)
3. A. F. G. Bourke, N. R. Franks, *Social Evolution in Ants* (Princeton Univ. Press, Princeton, NJ, 1995).
4. S. Camazine *et al.*, *Self-Organization in Biological Systems* (Princeton Univ. Press, Princeton, NJ, 2003).
5. E. J. H. Robinson, O. Feinerman, N. R. Franks, Flexible task allocation and the organization of work in ants. *Proc. Biol. Sci.* **276**, 4373 (2009). [doi:10.1098/rspb.2009.1244](https://doi.org/10.1098/rspb.2009.1244) [Medline](#)
6. J. M. Jandt, A. Dornhaus, Spatial organization and division of labour in the bumblebee *Bombus impatiens*. *Anim. Behav.* **77**, 641 (2009). [doi:10.1016/j.anbehav.2008.11.019](https://doi.org/10.1016/j.anbehav.2008.11.019)
7. C. R. Smith, A. L. Toth, A. V. Suarez, G. E. Robinson, Genetic and genomic analyses of the division of labour in insect societies. *Nat. Rev. Genet.* **9**, 735 (2008). [doi:10.1038/nrg2429](https://doi.org/10.1038/nrg2429) [Medline](#)
8. B. R. Johnson, Within-nest temporal polyethism in the honey bee. *Behav. Ecol. Sociobiol.* **62**, 777 (2008). [doi:10.1007/s00265-007-0503-2](https://doi.org/10.1007/s00265-007-0503-2)
9. T. D. Seeley, Adaptive significance of the age polyethism schedule in honeybee colonies. *Behav. Ecol. Sociobiol.* **11**, 287 (1982). [doi:10.1007/BF00299306](https://doi.org/10.1007/BF00299306)
10. M. Vonshak, A. Shlagman, *Isr. J. Entomol.* **39**, 165 (2009).
11. M. Fiala, “Comparing ARTag and ARToolkit Plus fiducial marker systems” HAVE 2005 (IEEE Intl. Workshop on Haptic Audio Visual Environments and their Applications, 2005).
12. Materials and methods are available as supplementary materials on *Science Online*.
13. M. Rosvall, C. T. Bergstrom, Maps of random walks on complex networks reveal community structure. *Proc. Natl. Acad. Sci. U.S.A.* **105**, 1118 (2008). [doi:10.1073/pnas.0706851105](https://doi.org/10.1073/pnas.0706851105) [Medline](#)
14. M. A. Seid, J. F. A. Traniello, Age-related repertoire expansion and division of labor in *Pheidole dentata* (Hymenoptera: Formicidae): A new perspective on temporal polyethism and behavioral plasticity in ants. *Behav. Ecol. Sociobiol.* **60**, 631 (2006). [doi:10.1007/s00265-006-0207-z](https://doi.org/10.1007/s00265-006-0207-z)
15. A. Lenoir, *Bull. Biol. Fr. Belg.* **2–3**, 80 (1979).
16. J. Mourier, J. Vercelloni, S. Planes, Evidence of social communities in a spatially structured network of a free-ranging shark species. *Anim. Behav.* **83**, 389 (2012). [doi:10.1016/j.anbehav.2011.11.008](https://doi.org/10.1016/j.anbehav.2011.11.008)
17. D. Lusseau *et al.*, Quantifying the influence of sociality on population structure in bottlenose dolphins. *J. Anim. Ecol.* **75**, 14 (2006). [doi:10.1111/j.1365-2656.2005.01013.x](https://doi.org/10.1111/j.1365-2656.2005.01013.x) [Medline](#)

18. B. Blonder, A. Dornhaus, Time-ordered networks reveal limitations to information flow in ant colonies. *PLoS ONE* **6**, e20298 (2011). [doi:10.1371/journal.pone.0020298](https://doi.org/10.1371/journal.pone.0020298)
19. P. Shannon *et al.*, Cytoscape: A software environment for integrated models of biomolecular interaction networks. *Genome Res.* **13**, 2498 (2003). [doi:10.1101/gr.1239303](https://doi.org/10.1101/gr.1239303) [Medline](#)
20. A. D. Briscoe, L. Chittka, The evolution of color vision in insects. *Annu. Rev. Entomol.* **46**, 471 (2001). [doi:10.1146/annurev.ento.46.1.471](https://doi.org/10.1146/annurev.ento.46.1.471) [Medline](#)
21. J. F. A. Traniello, Comparative foraging ecology of north temperate ants: The role of worker size and cooperative foraging in prey selection. *Insectes Soc.* **34**, 118 (1987).
[doi:10.1007/BF02223830](https://doi.org/10.1007/BF02223830)
22. S. Fortunato, Community detection in graphs. *Phys. Rep.* **486**, 75 (2010).
[doi:10.1016/j.physrep.2009.11.002](https://doi.org/10.1016/j.physrep.2009.11.002)